Available online at www.sciencedirect.com
SCIENCE DIRECT®
Physica B 362 (2005) 286–294
PHYSICA B
www.elsevier.com/locate/physb

Selection of intra- or inter-molecular multiple-quantum coherences in NMR of highly polarized solution

Xiaoqin Zhu[a], Zhong Chen[a,b,*], Shuhui Cai[a], Jianhui Zhong[b,1]

[a]*Department of Physics, State Key Laboratory of Physical Chemistry of Solid Surface, Xiamen University, Xiamen, Fujian 361005, PR China*

[b]*Departments of Radiology and Physics and Astronomy, University of Rochester, Rochester, NY 14642, USA*

Received 27 January 2005; received in revised form 25 February 2005; accepted 26 February 2005

Abstract

In highly polarized scalar-coupled liquid systems, nuclear magnetic resonance signals from multiple-quantum coherences (MQCs) may be formed by inter-molecular dipolar and/or intra-molecular scalar couplings. Selection of specific signals can simplify the spectra, which may help us understand the underlying physical mechanisms in complex coupled spin systems. In this paper, a pulse sequence with three selective radio-frequency (RF) pulses and phase cycling was designed for this purpose. For an I_pS_q ($p, q = 1, 2, 3, \ldots$) spin system, there are three kinds of MQC signals, which originate from intra-molecular I–S, inter-molecular I–S, and inter-molecular S–S (or I–I) coherences. These three kinds of signals can be detected separately by proper phase cycling of RF pulses, which is independent of coupling constants. The intra- and inter-molecular MQC signals can also be detected separately with specific preparation periods, but this method is sensitive to coupling constants. Our theoretical predictions are in good agreement with experimental observations. The method proposed herein can be extended to heteronuclear cases.

PACS: 76.60.−k; 76.80.+y; 75.40.Gb; 39.30.+w

Keywords: NMR; Inter-molecular MQCs; Intra-molecular MQCs; Dipolar couplings; Scalar couplings; Phase cycling

1. Introduction

The technique of multiple-quantum coherences (MQCs), has been developed rapidly for many important applications in magnetic resonance spectroscopy (MRS) and magnetic resonance imaging (MRI) [1–3]. Unique relaxation and diffusion properties of MQCs provide useful

*Corresponding author. Department of Physics, Xiamen University, Xiamen, 361005, PR China. Tel.: +86 592 2181712; fax: +86 592 2189426.

E-mail addresses: chenz@jingxian.xmu.edu.cn (Z. Chen), jianhui_zhong@urmc.rochester.edu (J. Zhong).

[1]Also for correspondence.

0921-4526/$ - see front matter © 2005 Elsevier B.V. All rights reserved.
doi:10.1016/j.physb.2005.02.026

information concerning molecular dynamics, which complements what can be derived from conventional single-quantum coherences (SQCs). MQCs can be used to simplify complex spectra and reveal some of the forbidden transitions in conventional single-quantum signals. With a sequence consisting of at least three radio-frequency (RF) pulses, conventional intra-molecular MQCs can be detected in the presence of scalar couplings in isotropic solution, or intra-molecular dipolar and/or quadrupolar couplings in anisotropic solution or solid with spin $\geqslant 1/2$ nucleus. A nuclear magnetic resonance (NMR) spectrum of a specific MQC order can be obtained by proper phase cycling [4,5], gradient field selection [6,7], or off-resonance excitation [8,9]. However, for highly polarized systems, COSY revamped by asymmetric z-gradient echo detection (CRAZED) sequence, which is composed of two RF pulses and proper field gradient pulses for coherence selection, can result in additional inter-molecular MQC peaks in the indirectly detected dimension of two-dimensional (2D) NMR spectra [10,11]. These peaks result from long-range dipolar interactions between distant spins in solution [12]. The phenomena of inter-molecular MQCs have been the subject of much interest recently in the NMR community [13,14]. They can be described with both quantum and classical treatments [15,16], which later have been demonstrated to be equivalent [17,18]. Combination of the quantum and classical treatments (so-called ''quantum-classical treatment'') may describe the experimental phenomena more easily in many cases [19].

Since the intra- and inter-molecular MQCs reflect different underlying physical processes, they have different apparent diffusion rates and relaxation properties [20–22]. In previous works, these two kinds of MQCs were always discussed separately. Most of the studies of inter-molecular MQCs were based on signals from a two-RF-pulse sequence, where no intra-molecular MQCs would be detected. Whereas when intra-molecular MQCs were detected with a sequence of at least three-RF pulses, inter-molecular dipolar couplings were always excluded, hence no inter-molecular MQCs were considered. However, this is not always justified. When a pulse sequence with more than two RF pulses is applied to a highly polarized scalar-coupled liquid system, NMR signals may originate from intra- and/or inter-molecular MQCs formed by intra-molecular scalar and/or inter-molecular dipolar couplings, respectively. Methods, capable of selecting specific intra- or inter-molecular MQC signals, may simplify the spectra and help us understand the underlying physical mechanisms [23,24]. To establish such methods, effective experimental schemes and theoretical analyses are highly desired. To the best of our knowledge, no effective methods for selecting intra- and inter-molecular MQC signals in highly polarized scalar-coupled liquid systems have been reported yet. In this paper, we limit our discussion to isotropic weakly coupled liquid system I_pS_q (p, $q = 1, 2, 3, \ldots$), where I and S are spin 1/2 nucleus. It is assumed that the intra-molecular dipolar couplings are averaged to zero due to molecular diffusion. A pulse sequence with three selective RF pulses shown in Fig. 1 is designed to separate MQC signals from intra-molecular I–S, or inter-molecular I–S, or inter-molecular S–S (or I–I) coherences. With proper phase cycling, these three kinds of signals can be selected, respectively. The theoretical predictions are compared with experimental observations.

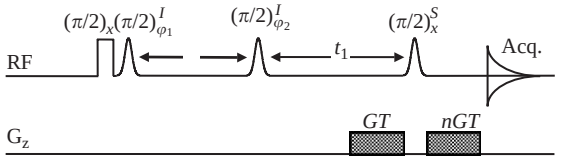

Fig. 1. Pulse sequence for selecting intra- and/or inter-molecular MQC signals. The first RF pulse is unselective, while the other three are selective for I, I, and S spins, respectively. Other parameters are defined in the text.

2. Theory and method

The pulse sequence shown in Fig. 1 was designed to select the signals originating from intra- and inter-molecular MQCs. The first $(\pi/2)_x$ RF pulse applied along the x-axis is unselective, and the other three RF pulses are selective for I, I, and S spins in turn, denoted as $(\pi/2)^I_{\varphi_1}$, $(\pi/2)^I_{\varphi_2}$,

and $(\pi/2)_x^S$, respectively. φ_1 and φ_2 are the phase shifts of the second and third RF pulses, respectively. With no interval between the first two RF pulses, $(\pi/2)_x(\pi/2)_{\varphi_1}^I$, are equivalent to $(\pi)_x^I(\pi/2)_{\varphi_1}^S$. A pair of linear gradients are applied along the z-axis with area ratio 1:n in order to select n-order MQCs, where G and T are the amplitude and duration, respectively, of the first gradient. Since there are more than two RF pulses in the sequence, signals from both intra- and inter-molecular MQCs may be detected [1,25].

Firstly, a homonuclear IS_2 spin system is chosen to demonstrate a theoretical description for the separate detection of intra- and inter-molecular MQCs in a highly polarized scalar-coupled liquid system, where I and S spins are scalar coupled to each other. The combination of the quantum and classical treatments was employed to treat the intra-molecular scalar couplings and inter-molecular dipolar couplings [26]. For simplification, effects of radiation damping, relaxation, and diffusion are disregarded in the following discussion. At first, the phase of the second and third pulses are applied along x direction for convenience. The density matrix at thermal equilibrium is given by [17,19]

$$\rho_{\mathrm{eq}} = 2^{-(N_I+N_S)} \prod_i (1 - \Im I_{iz}) \times \prod_{j,\beta} (1 - \Im S_{jz,\beta}), \tag{1}$$

where $\Im = 2\tanh(\hbar\omega_0/2kT)$; N_I and N_S represent the numbers of I and S spins, respectively; the indices i and j run over each molecule of the sample; the index β comes from multiple S spins in the system, which are 1 and 2 for the IS_2 spin system. The first two pulses, $(\pi/2)_x(\pi/2)_x^I$, convert the magnetization of S spins into y direction and the magnetization of I spins into $-z$ direction. During the preparation period τ, only coherences of S spins evolve in the first-order J couplings (proportional to $2I_{jz}S_{jz}$) and the chemical shift. The density operator just after the second selective pulse $(\pi/2)_x^I$ is

$$\begin{aligned}\rho(\tau, t_1 = 0) = {} & 2^{-(N_I+N_S)} \prod_i (1 - \Im I_{iy}) \\ & \times \prod_{j,\beta} \{1 + \Im[S_{jy,\beta} \cos(\Delta\omega_S\tau) \\ & - S_{jx,\beta} \sin(\Delta\omega_S\tau)]c(\tau) \\ & + 2\Im I_{jy}[S_{jx,\beta} \cos(\Delta\omega_S\tau) \\ & + S_{jy,\beta} \sin(\Delta\omega_S\tau)]s(\tau)\},\end{aligned} \tag{2}$$

where $c(\tau) = \cos(\pi J\tau)$ and $s(\tau) = \sin(\pi J\tau)$, (similar abbreviations will be adopted in the following text); J is the coupling constant between I and S spins; $\Delta\omega_S$ represents the resonance offset of S spins in rotating frame. The density matrix evolves under the scalar coupling, chemical shift, and gradient during period t_1. Right after the last $(\pi/2)_x^S$ pulse, the density matrix becomes

$$\begin{aligned}\rho(\tau, t_1, t_2 = 0) = {} & 2^{-(N_I+N_S)} \prod_i \{1 - \Im[I_{iy} \\ & \times \cos(\Delta\omega_I t_1 + \gamma GTs_i) \\ & - I_{ix} \sin(\Delta\omega_I t_1 + \gamma GTs_i)]c(t_1)^2 \\ & + \text{unobservable terms}\} \\ & \times \prod_{j,\beta} \{1 + \Im[S_{jz,\beta} \\ & \times \cos(\Delta\omega_S t_1 + \gamma GTs_j) \\ & - S_{jx,\beta} \sin(\Delta\omega_S t_1 + \gamma GTs_j)] \\ & \times \cos(\Delta\omega_S\tau)c(\tau)c(t_1) \\ & - 2\Im I_{jz}S_{jx,\beta} \cos(\Delta\omega_S t_1 + \gamma GTs_j) \\ & \times \cos(\Delta\omega_S\tau)c(\tau)s(t_1) \\ & - \Im[S_{jx,\beta} \cos(\Delta\omega_S t_1 + \gamma GTs_j) \\ & + S_{jz,\beta} \sin(\Delta\omega_S t_1 + \gamma GTs_j)] \\ & \times \sin(\Delta\omega_S\tau)c(\tau)c(t_1) \\ & + 2\Im I_{jz}S_{jx,\beta} \sin(\Delta\omega_S t_1 + \gamma GTs_j) \\ & \times \sin(\Delta\omega_S\tau)c(\tau)s(t_1) \\ & + 2\Im[I_{jy} \cos(\Delta\omega_I t_1 + \gamma GTs_j) \\ & - I_{jx} \sin(\Delta\omega_I t_1 + \gamma GTs_j)]S_{jz,\beta} \\ & \times \sin(\Delta\omega_S t_1 + \gamma GTs_j) \\ & \times \cos(\Delta\omega_S\tau)s(\tau)c(t_1) \\ & + 2\Im[I_{jy} \cos(\Delta\omega_I t_1 + \gamma GTs_j) \\ & - I_{jx} \sin(\Delta\omega_I t_1 + \gamma GTs_j)]S_{jz,\beta} \\ & \times \cos(\Delta\omega_S t_1 + \gamma GTs_j) \\ & \times \sin(\Delta\omega_S\tau)s(\tau)c(t_1) \\ & + \text{unobservable terms}\},\end{aligned} \tag{3}$$

where $\Delta\omega_I$ represents the resonance offset of I spins in rotating frame, (γGTs_i) and (γGTs_j) are the dephasing angles at the positions s_i and s_j due to the gradient, respectively, and γ is the gyromagnetic ratio. Since there are no further RF pulses and the coherence order will remain constant, only terms with non-vanishing contributions have been kept in Eq. (3). Since the scalar coupling terms commute with the other secular terms in the Hamiltonian including the dipolar field, after the evolution due to scalar couplings during the detection period t_2, the density operator can be written as

$$\begin{aligned}\rho(\tau,t_1,t_2) = 2^{-(N_I+N_S)}\prod_i\{1-\Im[I_{iy}&\\ \times\cos(\Delta\omega_I t_1+\gamma GTs_i)&\\ -I_{ix}\sin(\Delta\omega_I t_1+\gamma GTs_i)]c(t_1)^2c(t_2)^2&\\ +\text{unobservable terms}\}&\\ \times\prod_{j,\beta}\{1+\Im[S_{jz,\beta}\cos(\Delta\omega_S t_1+\gamma GTs_j)&\\ -S_{jx,\beta}\sin(\Delta\omega_S t_1+\gamma GTs_j)c(t_2)]&\\ \times\cos(\Delta\omega_S\tau)c(\tau)c(t_1)&\\ -\Im S_{jy,\beta}\cos(\Delta\omega_S t_1+\gamma GTs_j)&\\ \times\cos(\Delta\omega_S\tau)c(\tau)s(t_1)s(t_2)&\\ -\Im[S_{jx,\beta}\cos(\Delta\omega_S t_1+\gamma GTs_j)c(t_2)&\\ +S_{jz,\beta}\sin(\Delta\omega_S t_1+\gamma GTs_j)]&\\ \times\sin(\Delta\omega_S\tau)c(\tau)c(t_1)+\Im S_{jy,\beta}&\\ \times\sin(\Delta\omega_S t_1+\gamma GTs_j)&\\ \times\sin(\Delta\omega_S\tau)c(\tau)s(t_1)s(t_2)&\\ +\Im[-I_{jx}\cos(\Delta\omega_I t_1+\gamma GTs_j)&\\ -I_{jy}\sin(\Delta\omega_I t_1+\gamma GTs_j)]&\\ \times\sin(\Delta\omega_S t_1+\gamma GTs_j)&\\ \times\cos(\Delta\omega_S\tau)s(\tau)c(t_1)c(t_2)s(t_2)&\\ +\Im[-I_{jx}\cos(\Delta\omega_I t_1+\gamma GTs_j)&\\ -I_{jy}\sin(\Delta\omega_I t_1+\gamma GTs_j)]&\\ \times\cos(\Delta\omega_S t_1+\gamma GTs_j)&\\ \times\sin(\Delta\omega_S\tau)s(\tau)c(t_1)c(t_2)s(t_2)&\\ +\text{unobservable terms}\}.&\end{aligned}\tag{4}$$

When the inter-molecular dipolar interactions are treated as the classical dipolar field, the longitudinal and transverse magnetizations can be expressed by Eqs. (5) and (6), respectively.

$$\begin{aligned}M_z(t_1,t_2,s) = M_0^S\cos(\Delta\omega_S t_1+\gamma GTs+\Delta\omega_S\tau)&\\ \times c(\tau)c(t_1),&\end{aligned}\tag{5}$$

$$\begin{aligned}M^+_{total} = M_0^I[\mathrm{i}\exp(\mathrm{i}\Delta\omega_I t_1+\mathrm{i}\gamma GTs)c(t_1)^2c(t_2)^2&\\ +\exp(\mathrm{i}\Delta\omega_I t_1+\mathrm{i}\gamma GTs)&\\ \times\sin(\Delta\omega_S t_1+\gamma GTs+\Delta\omega_S\tau)&\\ \times s(\tau)c(t_1)c(t_2)s(t_2)]&\\ +M_0^S[\sin(\Delta\omega_S t_1+\gamma GTs+\Delta\omega_S\tau)c(\tau)&\\ \times c(t_1)c(t_2)+\mathrm{i}\cos(\Delta\omega_S t_1+\gamma GTs+\Delta\omega_S\tau)&\\ \times c(\tau)s(t_1)s(t_2)],&\end{aligned}\tag{6}$$

where $M_0{}^I$ and $M_0{}^S$ represent the equilibrium magnetization per unit volume of I and S spins, respectively. According to Eq. (5), the distant dipolar field is given by

$$B_d = -\frac{\Delta_s c(\tau)c(t_1)}{\gamma\tau_d^S}\cos(\Delta\omega_S t_1+\gamma GTs+\Delta\omega_S\tau),\tag{7}$$

where $\tau_d^S=(\gamma\mu_0 M_0^S)^{-1}$ is the dipolar demagnetizing time of S spins; $\Delta_s=[3(\hat{\boldsymbol{s}}\cdot\hat{\boldsymbol{z}})^2-1]/2$, in which the unit vector $\hat{\boldsymbol{s}}$ defines the direction of the coherence-selection gradients, and $\hat{\boldsymbol{z}}$ indicates the direction of the static magnetic field. Since the gradient field is oriented along the z direction in our case, that is $\hat{\boldsymbol{s}}=\hat{\boldsymbol{z}}$, we have $\Delta_s=1$. Finally, the transverse magnetizations of I and S spins after the evolution under the chemical shift, the second gradient ($n\gamma GTs$) and the distant dipole field during the detection period are given as

$$\begin{aligned}M^{I+} = M_0^I\{\mathrm{i}\exp(\mathrm{i}\Delta\omega_I t_1+\mathrm{i}\gamma GTs)c(t_1)^2c(t_2)^2&\\ +\frac{1}{2\mathrm{i}}\exp(\mathrm{i}\Delta\omega_I t_1+\mathrm{i}\gamma GTs)&\\ \times c(t_1)c(t_2)s(t_2)s(\tau)&\\ \times[\exp(\mathrm{i}\Delta\omega_S t_1+\mathrm{i}\gamma GTs+\mathrm{i}\Delta\omega_S\tau)&\\ -\exp(-\mathrm{i}\Delta\omega_S t_1-\mathrm{i}\gamma GTs-\mathrm{i}\Delta\omega_S\tau)]\}&\\ \times\exp(\mathrm{i}\Delta\omega_I t_2+\mathrm{i}n\gamma GTs)&\\ \times\sum_k\{\mathrm{i}^k J_k[-2t_2\Delta_s c(t_1)c(\tau)/3\tau_d^S]&\\ \times\exp(\mathrm{i}k\Delta\omega_S t_1+\mathrm{i}k\gamma GTs+\mathrm{i}k\Delta\omega_S\tau)\},&\end{aligned}\tag{8}$$

$$M^{S+} = \frac{1}{2}\,\mathrm{i}M_0^S[\exp(\mathrm{i}\Delta\omega_S t_1 + \mathrm{i}\gamma GTs + \mathrm{i}\Delta\omega_S\tau)c(t_1+t_2) - \exp(-\mathrm{i}\Delta\omega_S t_1 - \mathrm{i}\gamma GTs - \mathrm{i}\Delta\omega_S\tau)c(t_1-t_2)] \times c(\tau)\exp(\mathrm{i}\Delta\omega_S t_2 + \mathrm{i}n\gamma GTs) \times \sum_k [\mathrm{i}^k J_k(-t_2\Delta_s c(t_1)c(\tau)/\tau_d^S) \times \exp(\mathrm{i}k\Delta\omega_S t_1 + \mathrm{i}k\gamma GTs + \mathrm{i}k\Delta\omega_S\tau)]. \quad (9)$$

The effect of distant dipolar field B_d can be expressed by the following expansion, $\exp(\mathrm{i}\xi\cos\alpha) = \sum_{k=-\infty}^{\infty}\mathrm{i}^k J_k(\xi)\mathrm{e}^{\mathrm{i}k\alpha}$, where $J_k(\xi)$ is the Bessel function of integer order k and ξ is the argument of the Bessel function. For example, ξ equals to $-2t_2\Delta_s c(t_1)c(\tau)/3\tau_d^S$ in Eq. (8). In order to evaluate the signal of the whole sample, the average of the complex magnetization over all z positions was taken. If the size scale of a sample is much larger than dipolar correlation distance of spatial modulation, the spatial averaging across the sample retains only terms with $k = -n, -(n+1), -(n+2)$ in Eq (8) or $k = -n \pm 1$ in Eq. (9), independent of the absolute position in the sample. When $n = -2$, the resulting transverse magnetizations of I and S spins originating from intra-molecular I–S, inter-molecular I–S, and inter-molecular S–S double-quantum coherences (DQCs) can be written as

$$M_{\mathrm{intra}}^{I+} = \frac{1}{2\mathrm{i}}\,M_0^I\exp(\mathrm{i}\Delta\omega_I t_1 + \mathrm{i}\Delta\omega_S t_1)\exp(\mathrm{i}\Delta\omega_I t_2) \times \exp(\mathrm{i}\Delta\omega_S\tau)s(\tau)c(t_1)c(t_2)s(t_2), \quad (10)$$

and

$$M_{\mathrm{inter}}^{I+} \approx -\frac{1}{3}\,M_0^I\exp(\mathrm{i}\Delta\omega_I t_1 + \mathrm{i}\Delta\omega_S t_1) \times \exp(\mathrm{i}\Delta\omega_I t_2)(t_2\Delta_s/\tau_d^S)\exp(\mathrm{i}\Delta\omega_S\tau) \times c(\tau)c(t_1)^3c(t_2)^2, \quad (11)$$

from Eq. (8) and

$$M_{\mathrm{inter}}^{S+} \approx \frac{1}{4}\,M_0^S\exp(\mathrm{i}2\Delta\omega_S t_1)\exp(\mathrm{i}\Delta\omega_S t_2) \times (t_2\Delta_s/\tau_d^S)\exp(\mathrm{i}2\Delta\omega_S\tau)c(\tau)^2c(t_1) \times c(t_1+t_2) \quad (12)$$

from Eq. (9). Since most of our experiments satisfy the condition of small dipolar field effects, that is, $\xi \ll 1$, the Bessel functions in Eqs. (8) and (9) have been approximated to the first term of Tailor expansion $J_k(\xi) \cong (\xi/2)^k/k!$ [27]. Furthermore, when $\xi \ll 1$, the values of high-order Bessel functions are very small. Therefore, only zero- and first-order Bessel functions have been kept in Eqs. (10)–(12). Since the sample dimension in our experiments is much larger than the modulation length, $d = 2\pi/(\gamma GT)$, effects of sample shape can be neglected [16]. It can be seen that Eqs. (11) and (12) are related to the inter-molecular dipolar interactions ($t_2\Delta_s/\tau_d^S$). Therefore, they provide analytical expressions for signals originating from inter-molecular I–S and S–S DQCs, respectively. The chemical shift terms were ignored in the following discussion. Eq. (11) predicts that the I signal originating from inter-molecular I–S DQCs is proportional to $\cos(\pi J\tau)$, while Eq. (12) predicts that the S signal of spins originating from inter-molecular S–S DQCs is proportional to $\cos^2(\pi J\tau)$. Eq. (10) is independent of the inter-molecular dipolar interactions. It corresponds to the signal originating from conventional intra-molecular DQCs, which is proportional to $\sin(\pi J\tau)$. Therefore, when τ is set to $1/2J$, the signal from inter-molecular DQCs is zero. Eqs. (10)–(12) are reduced to

$$M_{\mathrm{intra}}^{I+} \approx \frac{1}{2\mathrm{i}}\,M_0^I\exp(\mathrm{i}\Delta\omega_I t_1 + \mathrm{i}\Delta\omega_S t_1) \times \exp(\mathrm{i}\Delta\omega_S/2J)\exp(\mathrm{i}\Delta\omega_I t_2)c(t_1) \times c(t_2)s(t_2), \quad (13)$$

$$M_{\mathrm{inter}}^{I+} = M_{\mathrm{inter}}^{S+} = 0. \quad (14)$$

There remains only the signal of I spins originating from intra-molecular DQCs. This result can be explained as follows: there is no distant dipolar field when τ is $1/2J$ (see Eq. (7)). Therefore, the signals originating from DQCs are induced by intra-molecular scalar couplings alone, and only signals originating from intra-molecular DQCs are induced when τ is set to $1/2J$. On the other hand, when τ equals $1/J$, the intensity of signal from intra-molecular DQCs is zero, and the resulting transverse magnetizations of inter-molecular DQCs are described as

$$M_{\mathrm{inter}}^{I+} \approx \frac{1}{3}\,M_0^I(t_2\Delta_s/\tau_d^S)\exp(\mathrm{i}\Delta\omega_I t_1 + \mathrm{i}\Delta\omega_S t_1 + \mathrm{i}\Delta\omega_S/J)\exp(\mathrm{i}\Delta\omega_I t_2)c(t_1)^3c(t_2)^2, \quad (15)$$

$$M_{\text{inter}}^{S+} \approx \frac{1}{4} M_0^S (t_2 \Delta_s/\tau_d^S) \exp(\mathrm{i}\Delta\omega_S t_2) \times \exp(\mathrm{i}2\Delta\omega_S t_1 + \mathrm{i}2\Delta\omega_S/J) \times c(t_1)c(t_1+t_2). \quad (16)$$

Eqs. (15) and (16) show that both I and S signals only originate from inter-molecular DQCs. Similarly, expressions of I and S signals originating from other orders of inter- or intra-molecular MQCs can be deduced when the quantum number n is set to a specific value. Although signals from intra- and inter-molecular MQCs may be separated by specific τ value for the preparation period when a single scalar coupling constant characterizes the system, the method is sensitive to the spin-coupling network and coupling constants in general.

For a more general spin system like I_pS_q (p, $q = 1, 2, 3, \ldots$), the resulting transverse magnetizations are

$$M_{\text{intra}}^{I+} = \frac{1}{2\mathrm{i}} M_0^I \exp(\mathrm{i}\Delta\omega_I t_1 + \mathrm{i}\Delta\omega_S t_1) \times \exp(\mathrm{i}\Delta\omega_I t_2) \exp(\mathrm{i}\Delta\omega_S \tau) c(\tau)^{p-1} s(\tau) \times c(t_1)^{q-1} s(t_1)^{p-1} c(t_2)^{q-1} s(t_2), \quad (17)$$

$$M_{\text{inter}}^{I+} \approx -\frac{1}{3} M_0^I \exp(\mathrm{i}\Delta\omega_I t_1 + \mathrm{i}\Delta\omega_S t_1) \times \exp(\mathrm{i}\Delta\omega_I t_2)(t_2 \Delta_s/\tau_d^S) \exp(\mathrm{i}\Delta\omega_S \tau) \times c(\tau)^p c(t_1)^{p+q} c(t_2)^q, \quad (18)$$

$$M_{\text{inter}}^{S+} \approx \frac{1}{4} M_0^S \exp(\mathrm{i}2\Delta\omega_S t_1) \exp(\mathrm{i}\Delta\omega_S t_2)(t_2 \Delta_s/\tau_d^S) \times \exp(\mathrm{i}2\Delta\omega_S \tau) c(\tau)^{2p} c(t_1)^p c(t_1+t_2)^p. \quad (19)$$

Eqs. (17)–(19) show that if the signals from inter-molecular DQCs are zero, the signal from intra-molecular DQCs is also zero when $p \geqslant 2$. It means that the signal from intra-molecular DQCs cannot be separated from the mixed signals of inter- and intra-molecular DQCs with specific τ value. To realize the separation, phase cycling was designed according to their coherence transfer pathways [28–30]. The coherence transfer pathways of the three kinds of signals originating from intra-molecular I–S, inter-molecular I–S, and inter-molecular S–S DQC are shown as (a), (b), and (c), respectively.

(a) $$S_z(l=0) \xrightarrow{(\pi/2)S_x} -S_y(l=-1) \xrightarrow{(\pi J\tau)2I_zS_z} 2I_zS_x(l=1) \xrightarrow[\Delta\omega t_1]{(\pi/2)I_x} -2I_yS_y(l=-2) \xrightarrow{(\pi/2)S_x} -2I_yS_z(l=-1),$$

(b) $$I_{iz}S_{jz}(l=0) \xrightarrow[(\pi)I_x]{(\pi/2)S_x} I_{iz}S_{jy}(l=1) \xrightarrow{(\pi J\tau)2I_zS_z} I_{iz}S_{jy}(l=1) \xrightarrow{(\pi/2)I_x} -I_{iy}S_{jy}(l=-2) \xrightarrow{(\pi/2)S_x} -I_{iy}S_{jz}(l=-1),$$

(c) $$S_{iz}S_{jz}(l=0) \xrightarrow{(\pi/2)S_x} S_{iy}S_{jy}(l=2) \xrightarrow{(\pi/2)I_x} S_{iy}S_{jy}(l=2) \xrightarrow[\Delta\omega t_1]{(\pi/2)S_x} -S_{ix}S_{jz}(l=-1),$$

where l is the coherence level. Table 1 shows the phase cycling schemes for selecting or suppressing these three kinds of DQC signals. Phase cycling scheme I is used to suppress signal from inter-molecular S–S DQCs; phase cycling scheme II is used to select signal from inter-molecular S–S DQCs; phase cycling scheme III is used to select signal from intra-molecular I–S DQCs; and phase cycling scheme IV is used to select signal from inter-molecular I–S DQCs.

Phase cycling scheme is independent of the number of spins (p and q). The combination of the preparation period interval τ selection and phase cycling will yield much better selections of the signals from one of the three pathways.

3. Experimental

Experiments were performed on a Varian Unity+ 500 spectrometer, equipped with self-shielded z-gradient coil and 5 mm HCN triple-resonance RF coil with 1.5 cm effective length. The pulse sequence is shown in Fig. 1. The gradient

Table 1
Phase cycling schemes for selecting specific signals

Phase cycling scheme	(I)		(III)			
φ_1	$+x$	$+x$	$+x$	$+x$	$-x$	$-x$
φ_2	$+x$	$-x$	$+x$	$-x$	$+x$	$-x$
Receiver phase	$+x$	$-x$	$+x$	$-x$	$+x$	$-x$
Phase cycling scheme	(II)		(IV)			
φ_1	$+x$	$+x$	$+x$	$+x$	$-x$	$-x$
φ_2	$+x$	$-x$	$+x$	$-x$	$+x$	$-x$
Receiver phase	$+x$	$+x$	$+x$	$-x$	$-x$	$+x$

amplitude $G \approx 0.1$ T/m and gradient duration $T = 1.2$ ms. The relaxation delay (RD) was 40 s to allow the spin system return to its full equilibrium state and prevent any possible stimulated echoes. The acquisition time was 1.8 s. To suppress the effect of radiation damping, the pulse width of the $\pi/2$ hard pulse was extended to 27.1 μs by deliberately detuning the probe. $\pi/2$ Gaussian pulse had the pulse width of 5.1 ms and $\pi/2$. A sample of 1,1,2-trichloroethane, $CHCl_2CH_2Cl$, dissolved in acetone-d_6 solvent (volume ratio 3:2) was used as an IS_2 system, where I and S spins represent the CH and CH_2 protons, respectively.

4. Results and discussion

Fig. 2(a) shows the 1D spectrum of 1,1,2-trichloroethane solution. The left one presents the I spin signal while the right one presents the S spin signal. The scalar coupling constant between I and S is 5.8 Hz. When the pulse sequence shown in Fig. 1 was applied without phase cycling, the signals originate from the intra-molecular, inter-molecular I–S, and inter-molecular S–S DQCs (see Fig. 2(b)). The I signal is composed of those originating from both intra- and inter-molecular I–S DQCs, and the S signal originates from inter-molecular S–S DQCs. Since the long-range dipolar field for a liquid sample is small, the signal intensities from the inter-molecular DQCs are usually much smaller than those from the intra-molecular ones [10]. Experimental result showed that the S signal is much smaller than the I signal. The amplitude variations of the three kinds of

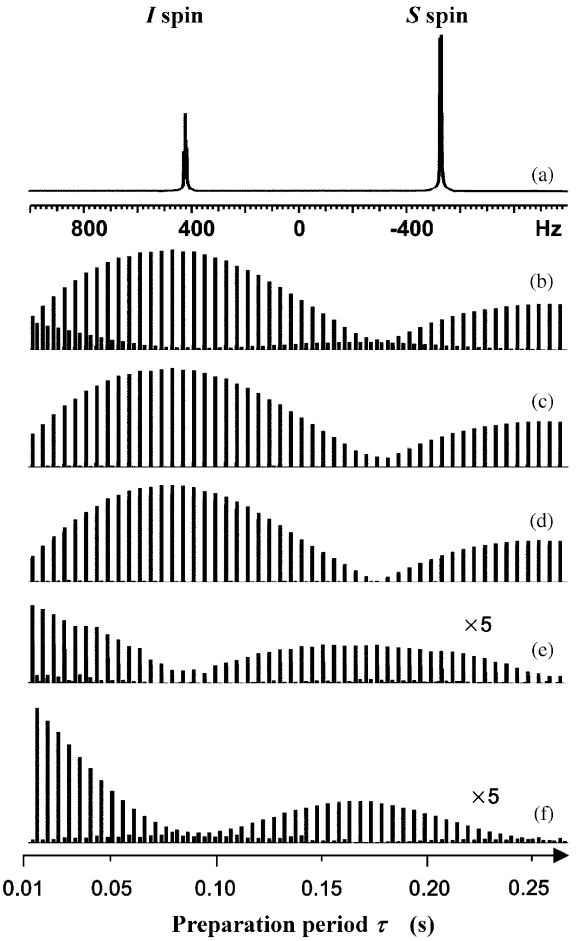

Fig. 2. (a) 1D spectrum of 1,1,2-trichloroethane using a single-pulse sequence. (b)–(f) Amplitudes of I and S signals varied with preparation period from 10 to 255 ms in an increments of 5 ms using the pulse sequence shown in Fig. 1. For each value of preparation period, both I and S peaks are plotted. The left one presents the I spin signal while the right one presents the S spin signal. (b) No phase cycling, (c) phase cycling scheme I, (d) phase cycling scheme III, (e) phase cycling scheme IV, and (f), phase cycling scheme II. Amplitudes were magnified 5 times in (e) and (f).

signals (two I spin signals are overlapped) are in good agreement with the theoretical predictions. With phase cycling scheme I, the signal from inter-molecular S–S DQCs was well suppressed, and the minimum of I signal was not equal to zero due to the existence of the inter-molecular I–S DQCs (see Fig. 2(c)). With phase cycling scheme III, only the

signal from intra-molecular DQCs was selected while the other signals were suppressed (see Fig. 2(d)). These results are similar to the ones obtained when the coherence-selection gradients are along magic angle direction or the sample is a dilute solution, where the dipolar field is close to zero and the inter-molecular DQCs (I–S and S–S) vanish. With phase cycling scheme IV, only the signal from inter-molecular $I-S$ DQC was selected (see Fig. 2(e)). With phase cycling scheme II, only the signal from inter-molecular S–S DQCs was selected (see Fig. 2(f)). The small residual signal of I spins in Figs. 2(e) and (f) may be due to the imperfect selective pulses and coherence-selection gradients. Work on suppressing the residual signal is in process. The attenuation of the signals varying with preparation period τ is caused by the effects of relaxation and diffusion.

5. Conclusion

In this paper, selection of signals originating from intra- and inter-molecular MQCs in a highly polarized I_pS_q (p, $q = 1, 2, 3, \ldots$) spin system were studied. When a pulse sequence with three selective pulses shown in Fig. 1 is used, three kinds of signals originate from intra-molecular I–S, inter-molecular I–S, and inter-molecular S–S or $I-I$ DQCs, respectively. A specific signal originating from intra- or inter-molecular MQCs may be selectively detected by adjusting the preparation period. However, this method is sensitive to the coupling networks and coupling constants. Theoretical analyses demonstrate that the coherence transfer pathway's of these three kinds of MQC signals are different. Therefore, they may be selected or suppressed by proper phase cycling, which is independent of the coupling constants. We have proposed some phase cycling schemes to select signal from a specific coherence transfer pathway and effectively suppress other undesired signals. The method may be extended to heteronuclear cases. Selection of different signals from intra- and/or inter-molecular MQCs helps us understand the underlying physical mechanisms in coupled spin systems.

Acknowledgements

This work was partially supported by the NNSF of China under Grants 10234070 and 10375049, and NIH under Grants NS32024 and NS41048.

References

[1] R.R. Ernst, G. Bodenhausen, A. Wokaun, Principles of Nuclear Magnetic Resonance in One and Two Dimensions, Clarendon Press, Oxford, 1987.
[2] W. Barros Jr., P.L. de Sousa, M. Engelsberg, J. Magn. Reson. 165 (2003) 175.
[3] A. Bifone, G.S. Payne, M.O. Leach, J. Magn. Reson. 135 (1998) 30.
[4] W.S. Warren, D.P. Weitekamp, A. Pines, J. Chem. Phys. 40 (1980) 581.
[5] S.S. Velan, P.T. Narasimhan, R.E. Jacobs, J. Magn. Reson. 152 (2001) 189.
[6] D.O. Cicero, G. Barbato, R. Bazzo, J. Magn. Reson. 148 (2001) 209.
[7] W.F. Reynolds, R.G. Enriquez, Magn. Reson. Chem. 39 (2001) 531.
[8] J.W. Logan, J.T. Urban, J.D. Walls, K.H. Lim, A. Jerschow, A. Pines, Solid State Nucl. Magn. Reson. 22 (2002) 97.
[9] T. Vosegaard, P. Florian, D. Massiot, P.J. Grandinetti, J. Chem. Phys. 114 (2001) 4618.
[10] W.S. Warren, W. Richter, A.H. Andreotti, B.T. Farmer II, Science 262 (1993) 2005.
[11] J.R. Owers-Bradley, O. Buu, C.J. Mc Gloin, R.M. Bowley, R. Konig, Physica B 284 (2000) 190.
[12] P.L. de Sousa, D. Gounot, D. Grucker, C. R. Chimie, 7 (2004) 311.
[13] C. Faber, E. Pracht, A. Haase, J. Magn. Reson. 161 (2003) 265.
[14] G.D. Charles-Edwards, G.S. Payne, M.O. Leach, A. Bifone, J. Magn. Reson. 166 (2004) 215.
[15] W. Richter, W.S. Warren, Concept. Magn. Reson. 12 (2000) 396.
[16] W.S. Warren, S. Lee, W. Richter, S. Vathyam, Chem. Phys. Lett. 247 (1995) 207.
[17] S. Lee, W. Richter, S. Vathyam, W.S. Warren, J. Chem. Phys. 105 (1996) 874.
[18] J. Jeener, J. Chem. Phys. 112 (2000) 5091.
[19] S. Ahn, S. Lee, W.S. Warren, Mol. Phys. 95 (1998) 769.
[20] J. Zhong, Z. Chen, E. Kwok, S.D. Kennedy, Magn. Reson. Imag. 19 (2001) 33.
[21] G. Tastevin, N. Piegay, F. Marion, P.J. Nacher, Physica B 329 (2003) 187.
[22] P.L. de Sousa, D. Gounot, D. Grucker. J. Magn. Reson. 162 (2003) 356.
[23] D. Balla, C. Faber, Chem. Phys. Lett. 393 (2004) 464.
[24] M.H. Levitt, R.R. Ernst, Chem. Phys. Lett. 100 (1983) 119.

[25] R. Freeman, Concept. Magn. Reson. 10 (1998) 63.
[26] R. Kimmich, NMR Tomography, Diffusometry, Relaxometry, Springer, Berlin, 1997.
[27] Z. Chen, Z.W. Chen, J.H. Zhong, J. Chem. Phys. 117 (2002) 8426.
[28] E.D. Minot, P.T. Callaghan, N. Kaplan, J. Magn. Reson. 140 (1999) 200.
[29] J.P. Marques, R. Bowtell, Magn. Reson. Med. 51 (2004) 148.
[30] S. Ahn, W.S. Warren, Chem. Phys. Lett. 291 (1998) 121.